$Er^{3+}/Yb^{3+}/Gd^{3+}$-TRIPLE-MODIFIED BISMUTH MOLYBDATE NANOSHEETS PHOTOCATALYST WITH ENHANCED PHOTOCATALYTIC ACTIVITY

Patrycja PARNICKA, Patrycja WILCZEWSKA, Adriana ZALESKA-MEDYNSKA

Department of Environmental Technology, University of Gdansk, Gdansk, Poland, EU
patrycja.parnicka@phdstud.ug.edu.pl

https://doi.org/10.37904/nanocon.2019.8697

Abstract

Semiconductor-based heterogeneous photocatalysis is a promising technology for water and air purification without using consumables and generating harmful by-products. Bismuth molybdate as one of the simplest Aurivillius oxides with a narrow band gap of 2.7 eV has got wide attention due to its potential for photocatalytic applications. However, the inherent disadvantages such as a fast recombination of photogenerated electron-hole pairs and slow charge carrier transfer leads to low photocatalytic efficiency. Recently, it was reported that modification with lanthanides ions greatly improves the separation efficiency and migration rate of the interface carrier. Therefore, we report a simple strategy for synthesis $Er^{3+}/Yb^{3+}/Gd^{3+}$ modified Bi_2MoO_6 vis hydrothermal method. The photocatalysts were characterized by diffuse reflectance spectroscopy (DRS), photoluminescence spectroscopy (PL) and scanning electron microscopy (SEM). The photocatalytic activity of the powder samples was assessed by the degradation of phenol in the liquid phase under ultraviolet and visible light irradiation. To provide insight into the reactive inviduals participating in the degradation mechanism, a test with scavengers was also performed. The composite photocatalysts exhibit remarkable enhancement of the photocatalytic activity during photocatalytic phenol degradation as compared with bare Bi_2MoO_6. These excellent photocatalytic performances are ascribed to the synergistic effects of the extended visible light response, and improved separation efficiency of the photoinduced charge carriers.

Keywords: Heterogeneous photocatalysis, bismuth molybdate, lanthanide ions

1. INTRODUCTION

One of the central global socio-economic challenges of the next decades is the sustainable treatment of wasted water and polluted air. Photocatalytic processes are regarded as a potential solution to this problem because they belong to the most sustainable and environmentally friendly technologies [1].

Bismuth molybdate is one of the simplest Aurivillius oxides possessing a layered structure with a regularly alternating bismuth $(Bi_2O_2)^{2+}$ and molybdenum $(MoO_4)^{2-}$ layers. Bi_2MoO_6 has an energy gap of ~ 2.7 eV and is characterized by the ability to create three-dimensional structures with a highly developed surface. In view of this, this photocatalyst can be successfully used to degrade environmental pollution using renewable energy sources such as solar radiation. Nevertheless, the inherent disadvantages such as a fast recombination of photogenerated electron-hole pairs and slow charge carrier transfer leads to low photocatalytic efficiency [2,3].

Recently, it was reported that modification with lanthanides ions greatly improves the separation efficiency and migration rate of the interface carrier. Based on the literature data, most of interest in lanthanide ions has focused on Er^{3+} due to their possible light absorption in the visible region [4]. In addition, Yb^{3+} ions are often used as sensitizer of Er^{3+} due to its particular electronic configuration, which creates the possibility of energy transfer between these ions [5]. The latest research presents the properties of Gd^{3+} ions which act as redox centers [6], generating strongly oxidizing hydroxyl radicals. The synergistic effect of Er-Yb-Gd ions may be effective approach to enhance the photocatalytic activity of Bi_2MoO_6.

Therefore, we report a simple strategy for synthesis $Er^{3+}/Yb^{3+}/Gd^{3+}$ modified Bi_2MoO_6 vis hydrothermal method. The aim of the work was to understand the effect of type of lanthanide ions on optical and luminescence properties and their relation with photocatalytic properties of bismuth molybdate.

2. EXPERIMENTAL SECTION

2.1. Preparation of $Er^{3+}/Yb^{3+}/Gd^{3+}$-modified bismuth molybdate

$Er^{3+}/Yb^{3+}/Gd^{3+}$ modified Bi_2MoO_6 photocatalysts were synthesized by hydrothermal method as described below: $Bi(NO_3)_3 \cdot 5H_2O$ (2 mmol) pre-dissolved in 80 mL water and 10 mL HNO_3 (20 mol/l) was dropwise added to 60 mL of $(NH_4)_6Mo_7O_{24} \cdot 4H_2O$ aqueous solution (0.14 mmol). After mixing for 30 min, the $Gd(NO_3)_3 \cdot 5H_2O$. $Er(NO_3)_3 \cdot 5H_2O$ and $Yb(NO_3)_3 \cdot 5H_2O$ was added. Then, 15 mL of ammonium hydroxide was added to adjust the pH to ~ 9 with a further continuous stirring for 30 min. The obtained suspension was transferred into 200 mL Teflon-linked stainless-steel autoclave and was maintained at 180 °C for 12 h. After cooling to room temperature, the resultant solid products were recovered by centrifugation. They were washed 3 times with distilled water and ethanol and dried at 60 °C overnight. The description of the as-prepared photocatalysts is summarized in **Table 1**.

Table 1 Description of obtained photocatalysts

Sample label	Assumed content of ytterbium (mol.%)	Assumed content of erbium (mol.%)	Assumed content of gadolinium (mol.%)
Bi_2MoO_6	none	none	none
Yb-Bi_2MoO_6	2	none	none
Er-Bi_2MoO_6	none	2	none
Gd-Bi_2MoO_6	none	none	2
Yb/Er-Bi_2MoO_6	2	2	none
Er/Gd-Bi_2MoO_6	none	2	2
Yb/Gd-Bi_2MoO_6	2	none	2
Yb/Er/Gd-Bi_2MoO_6	2	2	2

2.2. Characterizations

The morphology of prepared samples was characterized by field emission scanning electron microscopy (FE-SEM, JSM-7610F, JEOL). The diffuse reflectance spectra (DRS) of the samples were recorded on a Shimadzu UV-Vis spectrophotometer (UV 2600) equipped with an integrating sphere, with a wavelength range of 250-700 nm. The photoluminescence (PL) spectra were recorded by LS-50B Luminescence Spectrometer equipped with a Xenon discharge lamp and a R928 photomultiplier.

2.3. Photocatalytic measurements

The photocatalytic performance of $Er^{3+}/Yb^{3+}/Gd^{3+}$ modified Bi_2MoO_6 photocatalysts was investigated for phenol degradation under ultraviolet and visible light using a 1000W Xenon lamp (Oriel 66021) equipped with an optical filter (GG350) to cut-off the emission below 350 nm, and a water IR cut-off filter. Experiments were performed in a reactor at initial phenol and photocatalyst concentrations of 0.21 mM and 5 g/L, respectively. 0.2 mL phenol solution samples were taken every 20 min for 1 h, filtered using a syringe filter and then analyzed. A high-performance liquid chromatograph (HPLC, Shimadzu) equipped with a Kinetex C18 column and the SPD-M20A diode array detector (λ = 205 nm) was used to (150 x 3 mm; particle size of 2.6 μm; pore

diameter 100 Å) determine the phenol concentration in the solution. The mobile phase was composed of acetonitrile and 0.005% trifluoroacetic acid (20/80 v/v) with a constant flow rate equal to 0.5 mL/min. The injection volume was 20 µL. Radical scavenging experiments using benzoquinone, silver nitrate, ammonium oxalate and tert-butanol (solution of scavenger and phenol 1/1 C/C) were performed using the same procedure.

3. RESULTS

Scanning electron microscopy was used to characterize the morphology of the obtained $Er^{3+}/Yb^{3+}/Gd^{3+}$ modified Bi_2MoO_6 photocatalysts. **Figure 1** presents SEM images of selected samples. The obtained photocatalysts are characterized by an irregular sheet-like microstructure and a smooth surface. The size of nanosheet is about 1-4 microns.

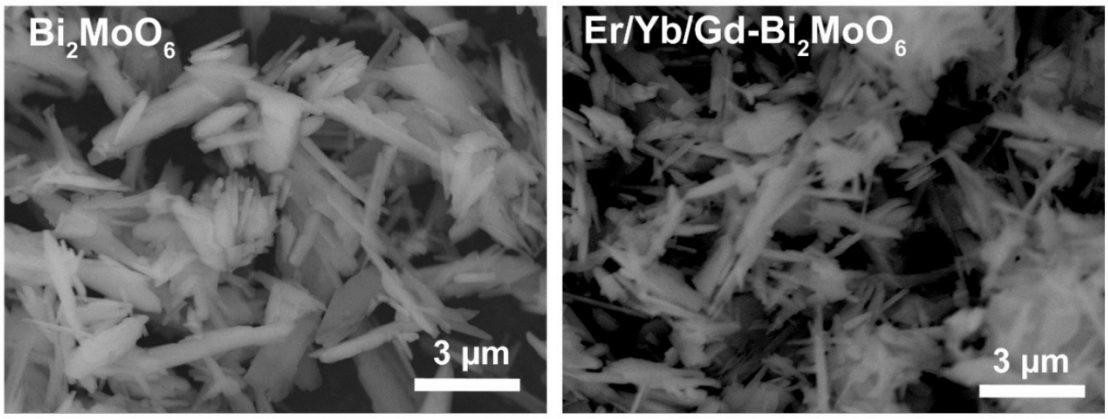

Figure 1 SEM images of bare Bi_2MoO_6 and Er/Yb/Gd-modified Bi_2MoO_6 photocatalysts

To investigate the photoabsorption properties of the obtained photocatalysts the diffusive reflectance spectra were recorded and data were converted by Kubelka-Munk function to obtain absorption spectra, and the results are shown in **Figure 2a**. All prepared photocatalysts were yellow powders. Each photocatalyst had a broad intense absorption below 415 nm. It can be seen, that all modified samples showed a redshift (shift in the direction of longer wavelengths) of their absorption compare to bare Bi_2MoO_6. The type of metal modification effects largeness of redshift. This behavior may be ascribed to the decrease in the band gap after modification of bismuth molybdate. Furthermore, there are three absorption bands in the Vis region typical for erbium located at 523, 545 and 674 nm. They correspond to transitions from the $^4I_{15/2}$ ground state to the excited states of $^4F_{7/2}$, $^4H_{11/2}$ and $^4F_{9/2}$. In all of the studied Er^{3+}-modified samples, the intensity of these absorption bands was similar. Nevertheless, the intensity of these absorption bands increases after co-modification Er^{3+} and Yb^{3+} ions.

To understand the rate of electron-hole recombination photoluminescence (PL) spectroscopy was applied. **Figure 2b** shows the PL spectra of bare and $Er^{3+}/Yb^{3+}/Gd^{3+}$ modified Bi_2MoO_6 photocatalysts under excitation by light at λ_{ex} = 350 nm. All samples show a broad emission band from 360 to 550 nm. It can be seen that the modification causes a reduction the photoluminescence intensity, which suggests significantly inhibited the recombination of the photogenerated charge carriers. The enhanced effect of separation of charge carriers is observed in the case of the triple-modified sample. In addition, it can be seen that erbium ions effectively inhibit the recombination process.

The photocatalytic properties of the obtained samples were investigated by observing the decomposition of phenol in an aqueous solution under UV-Vis (λ> 350 nm) light. Bare Bi_2MoO_6 were used as reference samples. The observed degradation rates (calculated for the 60 min of irradiation) are listed in **Table 2**. In turn the efficiency of phenol photodegradation is shown in **Figure 3a**.

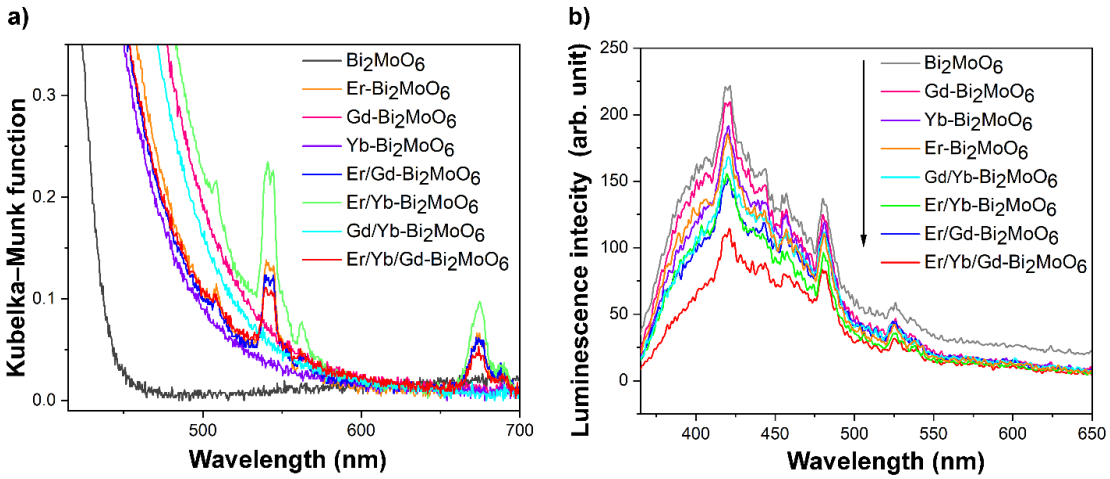

Figure 2 (a) UV-vis diffuse reflectance spectra; (b) Photoluminescence spectra of bare Bi_2MoO_6 and Er/Yb/Gd-modified Bi_2MoO_6 photocatalysts

Table 2 Photocatalytic activity under UV-Vis irradiation of bare Bi_2MoO_6 and Er/Yb/Gd-modified Bi_2MoO_6 photocatalysts

Sample label	Phenol degradation rate (min^{-1})	Intermediate products
Bi_2MoO_6	0.003	benzochinon hydrochinon
Yb-Bi_2MoO_6	0.007	
Er-Bi_2MoO_6	0.009	
Gd-Bi_2MoO_6	0.008	
Yb/Er-Bi_2MoO_6	0.018	
Er/Gd-Bi_2MoO_6	0.016	
Yb/Gd-Bi_2MoO_6	0.014	
Yb/Er/Gd-Bi_2MoO_6	0.035	

It was observed that all samples showed higher photoactivity than the reference sample. The phenol degradation rate constant increased from 0.003 to 0.035 min^{-1} for unmodified sample and triple-modified Bi_2MoO_6, respectively. Bi_2MoO_6 co-modified sample showed higher photocatalytic activity than single modified samples. However, the highest photoactivity was observed for the sample modified with erbium, ytterbium and gadolinium. After 90 min of irradiation, 96 % of phenol degraded in the presence of $Er^{3+}/Yb^{3+}/Gd^{3+}$-Bi_2MoO_6. There is a clear correlation between luminescence intensity and photocatalytic activity. HPLC analysis demonstrated that the main intermediates that formed during the photocatalytic degradation of phenol after 30 min under UV-Vis light were benzoquinone and hydroquinone. In addition, the amounts of intermediate products in the aqueous phase were observed to decrease during exposure on irradiation.

To confirm the role of generated of the reactive oxygen species in the photocatalytic process, the photocatalytic activity test in the water phase was conducted in the presence of obtained samples and scavenger. Ammonium oxalate, benzoquinone and tert-butyl alcohol were used as scavengers for h^+, $O2^{\bullet-}$ and $^{\bullet}OH$, respectively. As shown in **Figure 3b**, the photocatalytic systems containing ammonium oxalate completely inhibited phenol photodegradation. The research suggests that holes are the main active species in presented systems under UV-Vis irradiation. Moreover, phenol degradation efficiency also decreased significantly after addition of benzoquinone. This indicates that superoxide radicals also play an important role in the photocatalytic degradation of phenol.

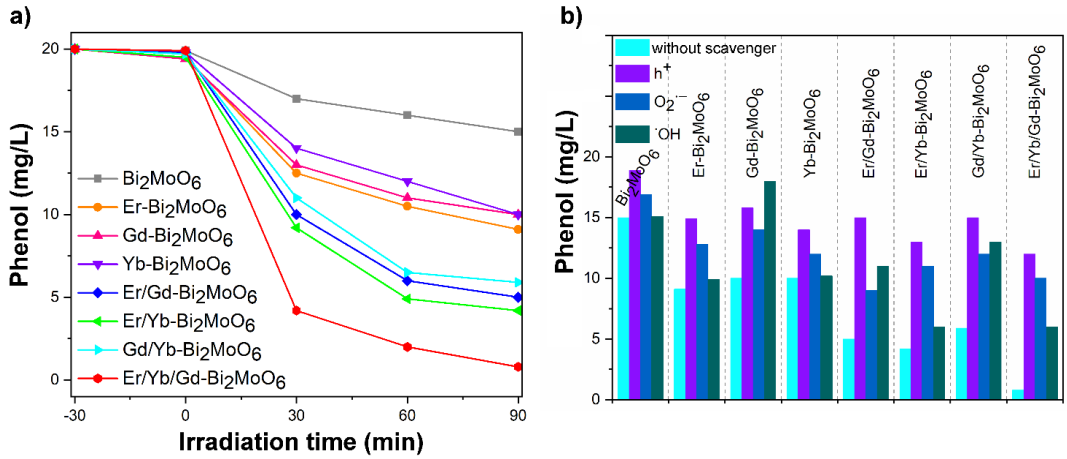

Figure 3 (a) Efficiency of phenol degradation under UV-Vis light irradiation of bare Bi_2MoO_6 and Er/Yb/Gd-modified Bi_2MoO_6 photocatalysts; (b) Photocatalytic degradation under UV-Vis light irradiation of phenol in the presence of photocatalysts and scavenger.

4. CONCLUSION

In summary, lanthanide modified bismuth molybdate was obtained by the hydrothermal method. The triple modified photocatalyst showed significantly increased photocatalytic activity compare to single and double modified Bi_2MoO_6 samples. After 90 min of UV-Vis irradiation, 96 % of phenol degraded in the presence of $Er^{3+}/Yb^{3+}/Gd^{3+}$-Bi_2MoO_6. Increased of photoactivity is attributed to the synergistic effect of $Er^{3+}/Yb^{3+}/Gd^{3+}$ ions. The introduction of Gd^{3+} ions in contributed to the hydroxyl radical´s generation, and further research indicated that the separation and transfer of electron-hole pairs were effectively promoted. In addition, Er^{3+}/Yb^{3+}-modification resulted in formation of an additional energy level, which led to the narrower band gap of Bi_2MoO_6, which greatly affected the visible light absorption property of the photocatalysts.

ACKNOWLEDGEMENTS

This research was financially supported by the program BMN (No. 538-8620-B297).

REFERENCES

[1] ZALESKA-MEDYNSKA, Adriana. Outlook and prospects, *Metal Oxide-Based Photocatalysis, Fundamentals and Prospects for Application*, Elsevier, 2018, pp. 341-344.

[2] NOUVELLES, Laboratoire D. C. and THOMAS, Avenue A., *The crystal chemistry and dielectric properties of the Aurivillius family of complex bismuth oxides with perovskite-like layered structures*, J. Alloys Compd. 188, 1992, pp. 27-35.

[3] JING, Kaiqiang, MA, Wen, REN, Yahang, XIONG, Jinhua, GUE, Binbin, SONG, Yujie, LIANG, Shijing and WU, Ling, *Hierarchical Bi_2MoO_6 spheres in situ assembled by monolayer nanosheets toward photocatalytic selective oxidation of benzyl alcoho*l, Appl. Catal. B Environ. 243, 2019, pp. 10-18.

[4] OBREGÓN, Sergio, KUBACKA, Anna, FERNÁNDEZ-GARCÍA, Marcos and COLÓN Gerardo, *High-performance Er^{3+}-TiO_2 system: Dual up-conversion and electronic role of the lanthanide*, J. Catal. 299, 2013, pp. 298-306.

[5] SALHI, Rached and DESCHANVRES, Jean L., *Efficient green and red up-conversion emissions in Er/Yb co-doped TiO_2 nanopowders prepared by hydrothermal-assisted sol-gel process*, J. Lumin. 176, 2016, pp. 250-259.

[6] LI, HONGDA, LI, WENJUN, WANG, FANGZHI, LIU, XINTONG, REN, CHAOJUN, MIAO, XIAO, *Fabrication of Pt nanoparticles decorated Gd-doped Bi_2MoO_6 nanosheets: Design, radicals regulating and mechanism of Gd/Pt-Bi_2MoO_6 photocatalyst*, Appl. Surf. Sci. 427, 2018, pp. 1046-1053.